



Contents lists available at ScienceDirect

Quaternary International

journal homepage: www.elsevier.com/locate/quaint

A tentative study of the relationship between annual $\delta^{18}\text{O}$ & δD variations of precipitation and atmospheric circulations—A case from Southwest China

Jing-Li Zhou ^a, Ting-Yong Li ^{a, b, *}

^a Chongqing Key Laboratory of Karst Environment, School of Geographical Sciences, Southwest University, Chongqing, 400715, China

^b Field Scientific Observation & Research Base of Karst Eco-environments at Nanchuan in Chongqing, Ministry of Land and Resources of China, Chongqing, 408435, China

ARTICLE INFO

Article history:

Received 8 November 2016

Received in revised form

9 May 2017

Accepted 22 May 2017

Available online xxx

Keywords:

Southwest China

Precipitation

Stable isotopes

ENSO

NAO

ABSTRACT

In this study, we present the 6-year $\delta^{18}\text{O}$ and δD records of precipitation from Chongqing, southwest China. Based on these data, the local meteoric water line (LMWL) has been set up as: $\delta\text{D} = 8.33\delta^{18}\text{O} + 19.42$. It is demonstrated that in El Niño scenarios, more vapor from closer moisture source (Western Pacific) was transported to south China, resulted in heavier stable isotopes of precipitation in southwest China, while in La Niña scenarios, the situations were just on the contrary. In addition, there is a positive correlation between the $\delta^{18}\text{O}$ of precipitation in southwest China and the Northern Atlantic Oscillation Index (NAOI) when the NAO is in the positive phase (typically in boreal winter-half year). At the interannual timescale, the $\delta^{18}\text{O}$ of precipitation in southwest China is more negative in strong NAO years than that in weak NAO years. We speculate that the north-south position migration of the westerlies and the route changes of vapor transport are correlated with the $\delta^{18}\text{O}$ changes of precipitation in southwest China under the climate change scenario around the North Atlantic.

© 2017 Elsevier Ltd and INQUA. All rights reserved.

1. Introduction

The stable isotope record of precipitation, reserved in ice cores, lacustrine sediments, tree-ring cellulose, speleothems, etc., is of great significance for the reconstruction of paleoclimate change. In recent years, the stalagmite $\delta^{18}\text{O}$ records have attracted considerable concern (Wang et al., 2001; Cheng et al., 2012; Duan et al., 2016), but the climatic significance of this proxy in Asian Monsoon regions is still contentious (Tan, 2016). The modern precipitation, as a crucial part in global water cycle, brings rich information on climate and environment. As the tracer of water cycle, the stable isotopic composition of precipitation, $\delta^{18}\text{O}$ and δD , is mainly controlled by the processes of evaporation and condensation, and influenced by many factors such as latitude, altitude, the distance from moisture source, temperature and rainfall. It is widely accepted that at various time scales, the isotopic composition in

precipitation can help us trace the origin of moisture source and the pathway of air mass transportation (Strong et al., 2007; Zhou et al., 2007; Coplen et al., 2008; Liu et al., 2010; Kebede and Travi, 2012; Stumpp et al., 2014; Wang et al., 2015). So, monitoring and analyzing the variation of precipitation isotopes in longer time scale (Eastoe and Dettman, 2016) and wider range (Lechler and Niemi, 2011) will be of benefit to the understanding of evolution process of general atmospheric circulation, and shed light on the value of paleoclimate reconstruction.

The relationship between δD and $\delta^{18}\text{O}$ in precipitation all over the world is called the Global Meteoric Water Line (GMWL), defined by Craig, revealing the internal relation between δD and $\delta^{18}\text{O}$ ($\delta\text{D} = 8\delta^{18}\text{O} + 10$) (Craig, 1961). The data from Global Network of Isotopes in Precipitation (GNIP), provided by the International Atomic Energy Agency (IAEA) confirm that the precipitation stable isotopic composition can be influenced by multiple factors. Before 1985, Hong Kong was the only monitoring station of GNIP in China; by 2015, there had been 33 stations in China. However, the data cannot be updated in time and are un-continuous except those collected in Hong Kong. It is particularly important to collect the original data in China considering the vast territory and the variety

* Corresponding author. School of Geographical Sciences, Southwest University, No. 2 Tiansheng Road, Beibei District, Chongqing, 400715, China.

E-mail address: cdlyt@swu.edu.cn (T.-Y. Li).

of natural environments. Inspired by the experience of GNIP, China set up the Chinese Network Isotopes in Precipitation (CHNIP) in 2004, based on the sites of Chinese Ecosystem Research Network (CERN) (Song et al., 2007). Southwest China is located to the east of the Tibet Plateau, influenced by the Indian Summer Monsoon (ISM), Eastern Asia Summer Monsoon (EASM), Asia Winter Monsoon (AWM), and the northern and southern branches of Westerlies (Fig. 1), which is even potentially influenced by the temperature changes in the southern hemisphere (Cheng et al., 2012; Li et al., 2014; Cai et al., 2015; Han et al., 2016; Zhang et al., 2017). But neither the GNIP nor CHNIP can provide data for this region. In this study, we collected monthly precipitation from January 2010 to December 2015 in Chongqing, southwest China, analyzed the stable isotopic composition of the precipitation, built the Local Meteoric Water Line (LMWL) and analyzed the seasonal and inter-annual variation of δD and $\delta^{18}O$ characteristics. Furthermore, we assessed the influence of circulation on the climate in southwest China by the integrated analysis of our data with the situations of El Niño, Southern Oscillation, North Atlantic Oscillation and the data of GNIP. Our work will make contribution to the defining of the climatic significance of Chinese stalagmite $\delta^{18}O$, which will promote both the reconstruction of paleoclimate in this region and the research on the evolution of the Asian monsoon.

2. Study area, data and method

2.1. Study area

Precipitation samples were collected in the campus of Southwest University (SWU), Beibei, Chongqing, southwest China

(29°49'N, 106°25'E, altitude: 252 m) (Fig. 1). This region is dominated by typical subtropical, humid monsoon climate. The prevailing monsoons in summer are ISM and EASM, while in winter it is AWM. In the rainy season from May to October, the rainfall accounts for 70%–80% of the total precipitation throughout the year. During the period from 2010 to 2015, mean annual temperature is 18.5 °C, average annual rainfall is 1119 mm, and annual average humidity is about 77% in Beibei.

2.2. Data and analyzing method

Following the standard method for the collection of stable isotopic samples of precipitation (<https://nucleus.iaea.org/wiser/index.php>) presented in GNIP operated by IAEA, we set up our collecting equipment (a barrel) of precipitation on the building roof of the school of Geographical Sciences in SWU with 5 mm thick liquid paraffin to avoid the evaporation of rainfall. And the barrel was packed with tinfoil and bubble paper to eliminate the solar radiation-induced chemical effect. We collected the samples at regular intervals of single month, so each sample represents one-month's precipitation. All samples were stored in low-temperature condition at 5 °C, and 5 ml rain water was taken for test every month.

The stable isotopic analysis was performed on the liquid water isotope analyzer (LWIA DLT-100), Los Gatos Research Company, USA. For each sample, 1.5 ml volume water was analyzed for six times, and the last four data were used to calculate the average as the result of the sample. Accuracy of measurement is $\pm 0.5\text{‰}$ for δD and $\pm 0.2\text{‰}$ for $\delta^{18}O$ (2σ), respectively. Final results were expressed in permil by the relative to Vienna Standard Mean Ocean Water (V-

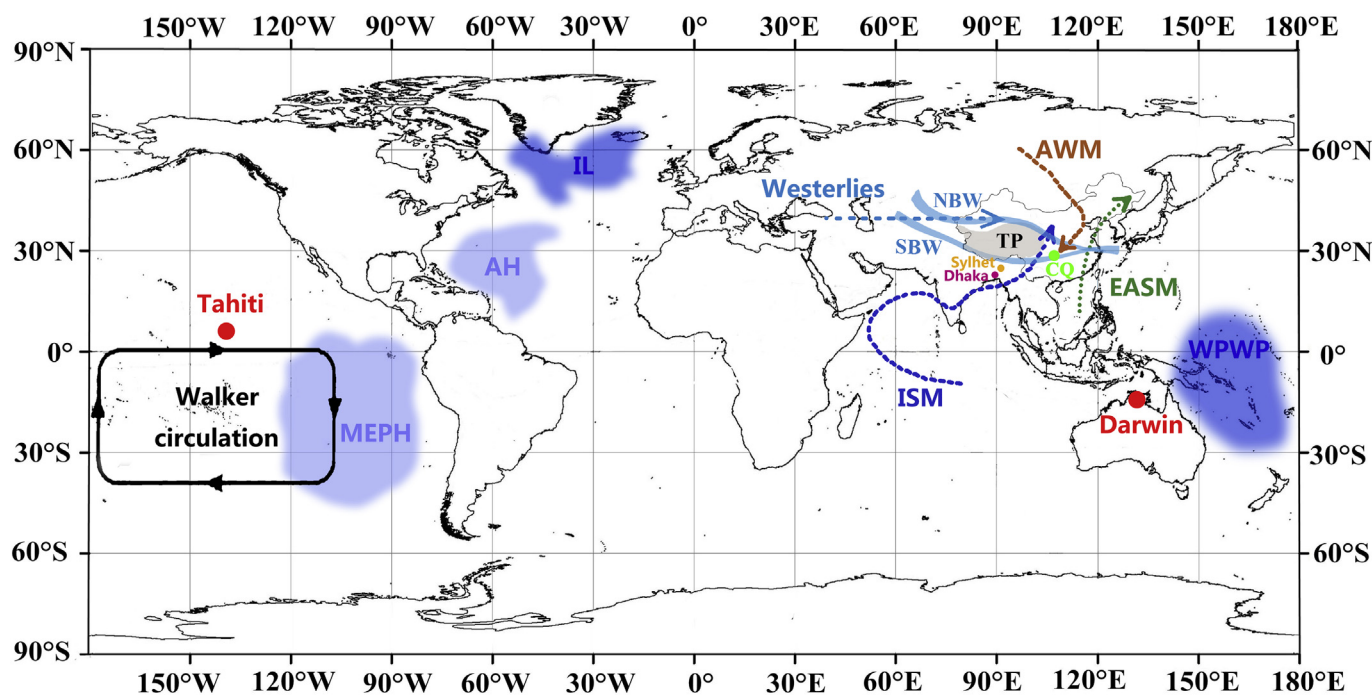


Fig. 1. (A) Location of the study site and the sketch map of the planetary circulations (After Cheng et al., 2012; Railsback et al., 2014). The gray area denotes the region of the Tibetan Plateau (TP). The light blue dashed line with arrow denotes the northern hemisphere westerlies. The light blue bands indicate the northern (NBW) and southern (SBW) branch of the westerlies around the Tibetan plateau. Dark blue dashed line with arrow indicates the Indian summer monsoon (ISM). Green dashed line with arrow denotes the East Asian Summer monsoon (EASM). Brown dashed line with arrow indicates the Asia Winter monsoon (AWM). The light blue areas present the Azores high (AH) and middle-east Pacific high (MEPH) and the blue areas denote the West Pacific warm pool (WPWP) and Icelandic low (IL) (after Marshall et al., 2001; Takahashi et al., 2009; Cane, 2005; Dvoryaninov et al., 2016). The coupled changes between these high and low cells result in the variation of North Atlantic oscillations (NAO) and El Niño-Southern Oscillations (ENSO). The light green solid circle presents the location of Chongqing (CO), Southwest, China. (For interpretation of the references to colour in this figure legend, the reader is referred to the web version of this article.)

SMOW) value:

$$\delta^{18}\text{O} = \left[\left(\frac{^{18}\text{O}}{^{16}\text{O}} \right)_{\text{sample}} - \left(\frac{^{18}\text{O}}{^{16}\text{O}} \right)_{\text{V-SMOW}} \right] / \left(\frac{^{18}\text{O}}{^{16}\text{O}} \right)_{\text{V-SMOW}} * 10^3\text{‰}$$

$$\delta\text{D} = \left[\left(\frac{\text{D}}{\text{H}} \right)_{\text{sample}} - \left(\frac{\text{D}}{\text{H}} \right)_{\text{V-SMOW}} \right] / \left(\frac{\text{D}}{\text{H}} \right)_{\text{V-SMOW}} * 10^3\text{‰}$$

In this study, we present the $\delta^{18}\text{O}$ and δD data of precipitation from January 2010 to December 2015 with data absent in August 2011 and in the period from May to August 2013 because of non sampling in unavoidable circumstances.

The data about the monthly average temperature and rainfall were provided by the Weather Bureau of Beibei district with 3 km distance and 20 m altitude difference from the sampling site. The other data referred to in this study were downloaded from the official websites as follows: Sea Surface Temperature Anomaly (SSTA) for the zone of Nino 3.4—<http://www.cpc.ncep.noaa.gov/data/indices/sstoi.indices>; Southern Oscillation Index (SOI)—<https://crudata.uea.ac.uk/cru/data/soi/soi.dat>; Global Network of Isotopes in Precipitation (GNIP)—<https://nucleus.iaea.org/wiser/index.php>; and Northern Atlantic Oscillation Index (NAOI)—<http://www.cpc.ncep.noaa.gov/products/precip/CWlink/pna/nao.shtml>.

3. Results and discussion

3.1. Local meteoric water line (LMWL)

In the monitoring period, the δD and $\delta^{18}\text{O}$ values of precipitation varied from 36‰ to –122‰ and from 0.6‰ to –16.8‰, respectively, falling into the variation range of global precipitation, and the most positive and negative values occurred in January 2013 and September 2011, respectively. The LMWL of Chongqing is presented as $\delta\text{D} = 8.33\delta^{18}\text{O} + 19.42$ ($n = 65$, $r = 0.979$, $p < 0.001$) (Fig. 2). We also presented a LPWMWL (Local precipitation weighted meteoric water line) as $\delta\text{D} = 8.30\delta^{18}\text{O} + 16.60$ ($n = 65$, $r = 0.983$, $p < 0.001$) (Fig. 2), which is mentioned by Hughes and Crawford (2012), with a

minimum effect of small precipitation samples on the calculation of the LMWL. The slope and intercept of Chongqing LMWL and LPWMWL are larger than those of the GMWL ($\delta\text{D} = 8\delta^{18}\text{O} + 10$) (Craig, 1961) and the Chinese Water Meteoric Water line (CMWL) ($\delta\text{D} = 7.9\delta^{18}\text{O} + 8.2$) (Zheng et al., 1983). This is because that the GMWL and CMWL were produced by the combined analysis of the data worldwide and the whole China, respectively. It is in fact present the average situation for various natural environments, including both the humid and arid regions. Chongqing is located in the monsoon area and dominated by humid climate, resulting in the relative larger slope and intercept of the LMWL. In addition, the slope and intercept of Chongqing LMWL are slightly larger than those of the LMWL of Hong Kong ($\delta\text{D} = 8.13\delta^{18}\text{O} + 11.39$) (Zhang et al., 2009a), which should be attributed to the difference in the molecular mass of isotope hydrogen and oxygen. During the transportation of moisture, the enrichment of deuterium is more than that of oxygen, because the fractionation rate of hydrogen is larger than that of oxygen (Li et al., 2010). Moreover, the moisture source of Hong Kong is mainly from West Pacific Ocean, but there are multi sources for Chongqing (mainly from Indian Ocean during summer months) (Ding and Liu, 2008; Yang et al., 2016) which leads to the difference in slope and intercept for the LMWL of each site.

3.2. Relationships between $\delta^{18}\text{O}$, monthly average temperature and rainfall amount

There is a negative correlation between the $\delta^{18}\text{O}$ and monthly average temperature in Chongqing ($\delta^{18}\text{O} = -0.15T - 0.32$, $r = -0.519$, $n = 65$, $p < 0.01$) (Fig. 4A), and the correlation coefficient in summer is larger than that in winter (Fig. 4C and E). This correlation is contrary to the “temperature effect”, which means a positive correlation between the precipitation $\delta^{18}\text{O}$ and temperature (Dansgaard, 1964), being more evident in the Northwest China, North China, and northern Tibet Plateau, with negative $\delta^{18}\text{O}$ values

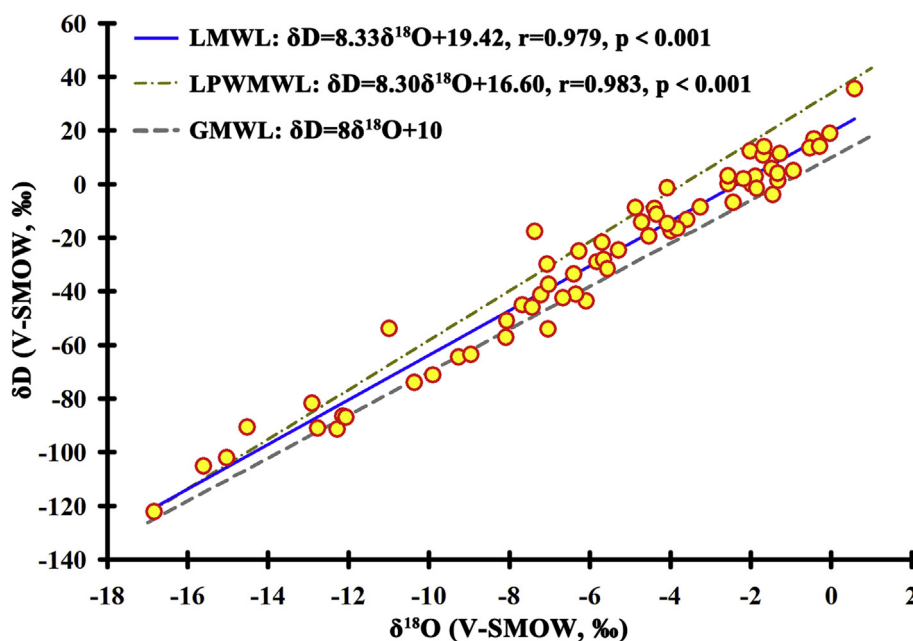


Fig. 2. Relationship between the $\delta^{18}\text{O}$ and δD values in the precipitation of Chongqing, Southwest China. The LMWL (Local meteoric water line) (blue line) and LPWMWL (Local precipitation weighted meteoric water line) (dashed brown line) have been plotted. The Global Meteoric water line (GMWL) (Dashed gray line) (Craig, 1961) has been presented for comparison. (For interpretation of the references to colour in this figure legend, the reader is referred to the web version of this article.)

in winter precipitation and positive values in summer rain water (Liu et al., 2008). This negative correlation is consistent with the conclusions from other monsoon regions of southern China (Liu et al., 2010). Because as a city in southwest China, there are at least two different moisture sources for Chongqing, named oceanic moisture in summer and continent moisture in winter. In other words, the “source effect” surpasses the influence of temperature, especially during the summer monsoon dominated months (Li et al., 2010).

There is a negative correlation between the $\delta^{18}\text{O}$ and rainfall amount ($\delta^{18}\text{O} = -0.02P - 3.78$, $r = -0.400$, $n = 65$, $p < 0.01$) (Fig. 4B). This negative correlation is presented for precipitation in winter too (Fig. 4F). But there is no obvious correlation between the $\delta^{18}\text{O}$ and rainfall amount for summer precipitation (Fig. 4D), which is consistent with previous conclusion that there is no obvious correlation between the $\delta^{18}\text{O}$ and rainfall inland (Zhang et al., 2004). The composition of stable isotopes in precipitation can be affected by many factors, such as the moisture source and atmospheric circulation (Rozanski et al., 1993). If there is a long distance from the moisture source, condensation and isotope fractionation may occur in the course of moisture transportation, which makes the stable isotopic composition of precipitation in the downstream lighter than that of the original moisture source (Hoffmann et al., 2000). In the summer monsoon prevailing months, even with less precipitation, the value of $\delta^{18}\text{O}$ is lighter than those in other months with large amounts of rain. For example, monthly precipitations of August and September in 2010 are only 56 mm and 90 mm, but the values of $\delta^{18}\text{O}$ are -15.6‰ and -12.9‰ , respectively. While during the pre-summer monsoon season, in April and May, 2010, the values of $\delta^{18}\text{O}$ are -4.9‰ and -4.4‰ , with the rainfall being as much as 130 mm and 117 mm, respectively (Fig. 3). It is proved that in Chongqing region, on the time scale of month and season, the isotopic composition of precipitation is mainly dominated by the change of moisture source and the degree of isotope fractionation during the transportation of moisture, rather than the absolute rainfall (Zhang et al., 2004; Li et al., 2010). The most positive $\delta^{18}\text{O}$ value of Chongqing precipitation occurred in spring before the rainy season, because of the enrichment effect of isotope fractionation by the evaporation of droplet during the falling of rain water in warm and dry weather.

3.3. *d*-excess

The term of *d*-excess, firstly defined by Dansgaard (1964) as $d\text{-excess} = \delta\text{D} - 8\delta^{18}\text{O}$, demonstrates the degree of deviation from the equilibrium of isotopic fractionation caused by the kinetic fractionation during the evaporation of vapor. *d*-excess reflects the thermal conditions and the situation of vapor balance when the air mass being formed (Merlivat and Jouzel, 1979). It also records the climatic conditions such as temperature, humidity and supersaturated environment when the rainfall happened (Deshpande et al., 2013). Based on the analysis of *d*-excess, Tian et al. (2007), argued the northward maximum extent of the southwest monsoon over the Tibetan Plateau and the pattern of moisture transport. The *d*-excess of precipitation had also been used to explore the moisture source and the change of air masses in different season (Wang et al., 2015). Therefore, this proxy can be used to trace the meteorological conditions of moisture source which formed the precipitation (Pang et al., 2005). In this study, the values of *d*-excess ranged from 2‰ to 41‰, with the average being 18‰, which is obviously larger than the value of 10‰ for the global precipitation. It should be attributed to the isotopic fractionation during the processes of vapor evaporation and condensation, as a result of a long-distance

transportation of moisture from oceans (Fritz et al., 1987). There are negative correlations both between the *d*-excess and temperature (T), and between the *d*-excess and precipitation (P) (Fig. 3), with the linear equations being $d\text{-excess} = -0.71T + 30.15$ ($r = -0.671$, $n = 65$, $p < 0.01$), and $d\text{-excess} = -0.05P + 21.94$ ($r = -0.500$, $n = 65$, $p < 0.01$), respectively. In general, the *d*-excess values of Chongqing precipitation tend to decrease in summer and increase in winter, which can be attributed to the regional climatic feature. During the summer months with high temperature in southwest China, including Chongqing area, it is dominated by the summer monsoon (Fig. 1), with the mass of moisture being originated from the low-latitude oceans, resulted in high humidity and heavy precipitation with light *d*-excess values. While in winter (dry season), the regional climate is controlled by continental air mass (Fig. 1), and the moisture of precipitation is mainly supplied by the westerlies and the second evaporation under the cloud (Tian et al., 2005). The evaporation leads to kinetic fractionation of the stable isotopes (Deshpande et al., 2013), resulting in lower humidity and higher *d*-excess values (Zhang et al., 2009a, b; Chen et al., 2015). From the above analysis, the seasonal variation of *d*-excess in Chongqing precipitation is mainly controlled by different moisture source (Li et al., 2010).

3.4. Isotopic composition of precipitation in Chongqing and atmospheric circulations

3.4.1. Effects of ENSO on precipitation in Chongqing

ENSO is a generic term of El Niño and Southern Oscillation, which is a result of the large-scale atmosphere-ocean interaction (Neelin et al., 1998), leading to many climatic events, e.g. the extreme precipitation events, abnormal temperature and the deviation of the Intertropical Convergence Zone (ITCZ) (Bjerknes, 1969; Cane, 2005; Takahashi et al., 2009; Ham and Kug, 2014). The SSTA of the Niño 3.4 zone (5°N – 5°S , 170°W – 120°W) (Trenberth, 1997) and the SOI have been integrated as the proxy of ENSO, and there is a negative correlation between SSTA and SOI (Ropelewski and Jones, 1987). El Niño is going to happen when SOI maintains a negative value, or the La Niña is going to happen (Allan et al., 1991). Based on this determination, 2011 is a typical year of La Niña because of the positive value of SOI and 2015 is a typical year of El Niño (Fig. 5).

ENSO leads to the large-scale change of atmospheric circulations in the Northern Hemisphere and enlarges the influencing extent by dynamic and thermal effects. In lower troposphere, there is a teleconnection between the middle-east Pacific and East Asia during the mature stage of ENSO in boreal winter to the declining phase in boreal early summer of the next year, and the SSTA of middle-east Pacific exerts influences on the East Asia through the movement of the anticyclone in the northwest Pacific (Wang et al., 2000). The annual precipitation in 2011 (La Niña year) in Chongqing is 910 mm, with the weighted average δD and $\delta^{18}\text{O}$ values being -43‰ and -6.9‰ , respectively. While in 2015 (El Niño year), the annual precipitation is 1312 mm, with the weighted average δD and $\delta^{18}\text{O}$ value being -37‰ and -6.2‰ , respectively. Although the rainfall in 2015 is 40% more than that in 2011, the stable isotope composition is heavier than that of 2011, consistent with the trend of SOI variation, which is also corresponding to the lower SOI in 2015 compared with that in 2011 (Fig. 5).

In the situation of La Niña, the enhanced middle-east Pacific High increased the gradient of air pressure between the western and eastern Pacific, strengthening the Walker circulation and the southeast trade winds, which go across the equator, deflecting to the northeast and strengthening the India monsoon. As a result,

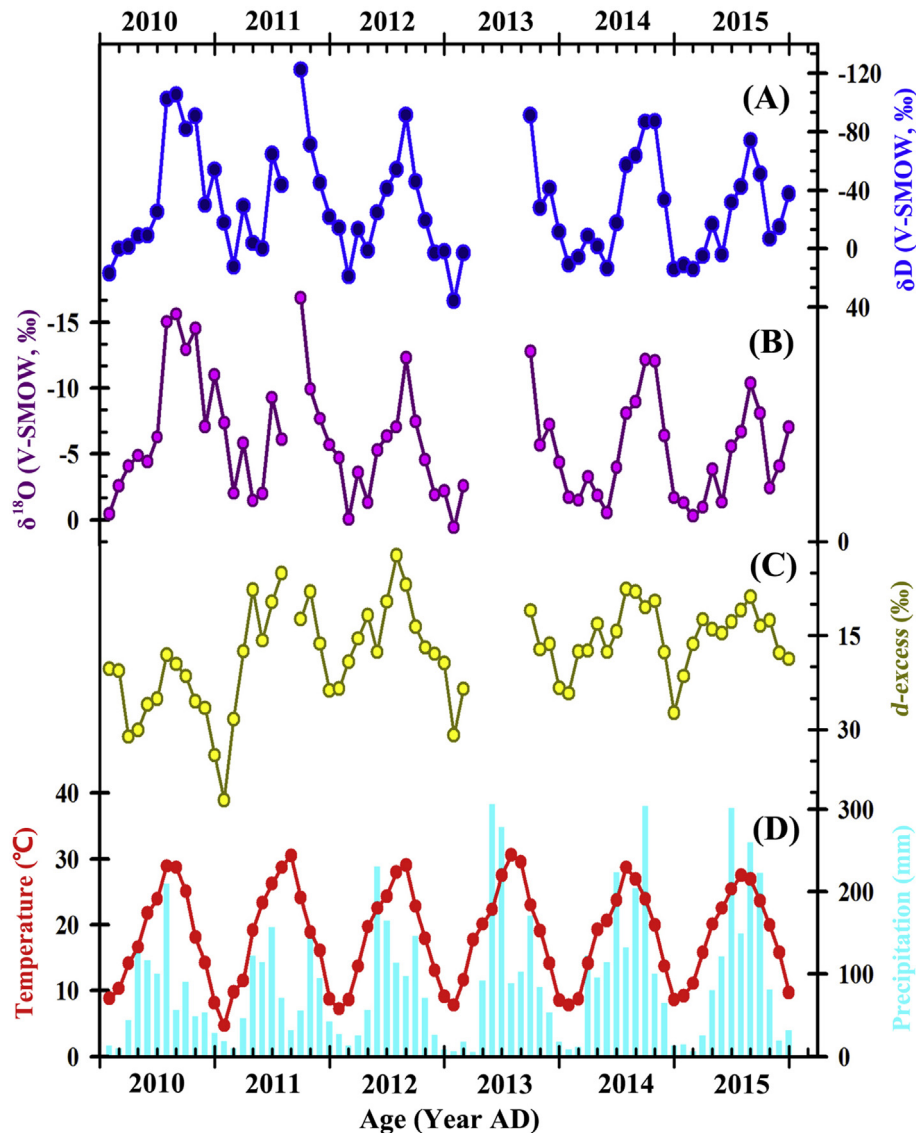


Fig. 3. The seasonal change of δD (A: blue line), $\delta^{18}O$ (B: purple line) and d -excess (C: yellow line) values and the monthly temperature (D: red line) and precipitation (D: light blue histogram) in Chongqing, Southwest China. (For interpretation of the references to colour in this figure legend, the reader is referred to the web version of this article.)

there is a rise in the component of moisture source from India Ocean with a lighter isotopic composition in the precipitation of Chongqing because of the long-distance transport (Tan, 2014). On the contrary, in the El Niño scenarios, the rising SST in the middle-east Pacific reduces the gradient of air pressure between the western and eastern Pacific, depresses the Walker circulations and sometimes can even lead to a reverse circulation over the tropical ocean zone. The strengthened East Asian Summer monsoon brings more vapor from the west Pacific, resulting in the heavy $\delta^{18}O$ values in the precipitation of Chongqing (Zhou and Yu, 2005; Tan, 2009).

3.4.2. Teleconnection between the precipitation in Chongqing and the NAO

NAO is a large-scale “seesaw” structure reflecting the variation of air mass between the subpolar low (Iceland Low, IL) and the subtropical high (Azores high, AH) in the region of North Atlantic (Fig. 1) (Walker, 1925; Serreze et al., 1995). The enhanced NAO will strengthen the westerlies, and vice versa (Rogers, 1984; Dvoryaninov et al., 2016). Changes of NAO have an enormous

influence on precipitation, temperature and the ecosystem of the northern hemisphere (Marshall et al., 2001). The winter precipitation in southwest China is mainly influenced by the teleconnection between the atmospheric circulations from the Mediterranean Areas (Brandimarte et al., 2011), Caspian Sea (Peng et al., 2002) to the Middle East-Arabian sea-Tibet Plateau (Liu and Yin, 2001; Cui et al., 2015), and its lower reaches. The winter NAO correlates to the climate of East Asian mainly by the Asian Torrent (Watanabe, 2004). There is an asymmetric positive correlation between the Southwest Rain Index (I_{SWR} , which reflect the amount of winter precipitation in Southwest China) and NAOI. In other word, the positive correlation only exists during the negative phase of NAOI, and there is no significant correlation between the I_{SWR} and NAOI when the latter is in the positive phase (Xu et al., 2012). In addition, there is a constant and significant teleconnection between the I_{SWR} and the sea level pressure of the North Atlantic, the Arabia Sea and the Bay of Bengal, especially in the winter months (Xu et al., 2012).

Based on the definition of strong and weak NAO year by Liu and

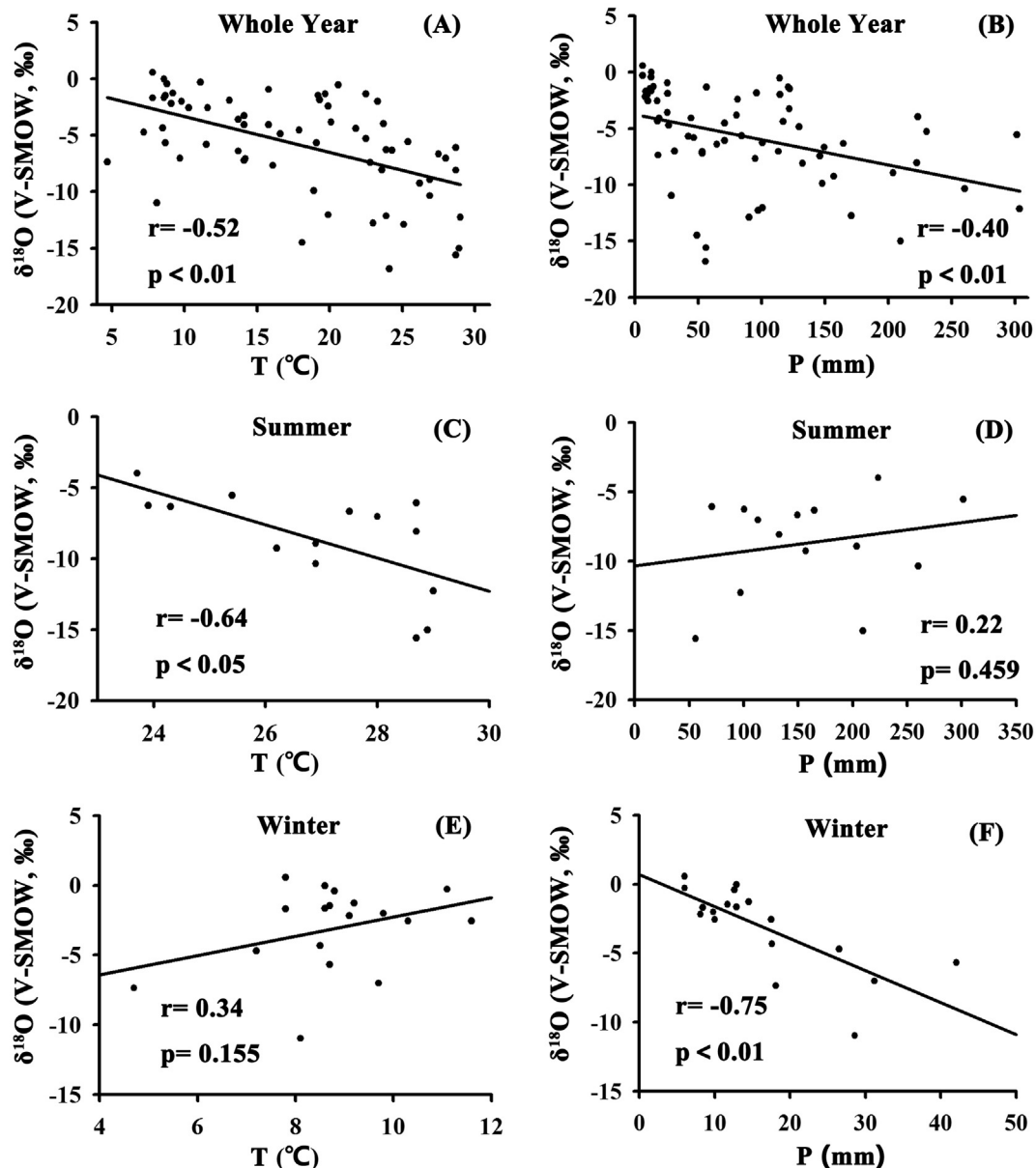


Fig. 4. The scatter plots between $\delta^{18}\text{O}$ and the monthly temperature(T)/precipitation(P) for whole year, (A): $\delta^{18}\text{O}$ vs T, (B): $\delta^{18}\text{O}$ vs P; summer months (June, July, August), (C): $\delta^{18}\text{O}$ vs T, (D): $\delta^{18}\text{O}$ vs P; winter months (December, January, February), (E): $\delta^{18}\text{O}$ vs T, (F): $\delta^{18}\text{O}$ vs P, respectively, in Chongqing, Southwest China.

Duan (2012), we calculated the standard deviation of NAOI in winter months (November, December and next January) from 2010 to 2015, and found that the standard deviation of NAOI was above 1 during 2010–2011 (strong year), while it was less than 1 during 2012–2015 (weak year). In 2010 and 2011, the weighted average values of $\delta^{18}\text{O}$ in winter precipitation ($\delta^{18}\text{O}_{\text{WP}}$) are -6.7‰ and -6.0‰ , respectively. However, the values became -1.2‰ , -4.4‰ , -3.1‰ , -5.6‰ in the NAO weak years (2012–2015). The average value of $\delta^{18}\text{O}_{\text{WP}}$ is obviously heavier in the NAO weak years than that in the NAO strong years (Liu and Duan, 2012). The correlation coefficient between the average value of $\delta^{18}\text{O}_{\text{WP}}$ and the standard deviation of NAOI in winter, $r = 0.812$, confirmed the significant correlation between them. In the NAO strong years, the water-vapor flux in the northern branch of the Tibetan plateau increased while the flux in the southern branch of the Tibetan plateau decreased. Situations in NAO weak years are on the contrary (Liu and Duan, 2012).

Under the influence of prevailing westerly jet, the Southern Branch Jet Stream (SBJS) of the Tibetan plateau brings moisture to southwest China (Fig. 1), influencing the moisture composition of local precipitation. The moisture of the SBJS comes from the Bay of Bengal, with heavier isotopic composition than the moisture of the northern branch, which comes from inland and experiences series of isotope fractionation processes (Tian et al., 2001). In conclusion, in the NAO strong years (e.g. 2010–2011), the lighter stable isotopic composition of precipitation in southwest China should be attributed to the decreasing flux of the SBJS (with heavier isotopic composition).

There is a positive relationship between the $\delta^{18}\text{O}$ of precipitation in Chongqing and the NAOI during the positive phase of NAOI in boreal winter (Fig. 6). From September 2011 to May 2012, there is a one-month lag and a similar trend between the $\delta^{18}\text{O}$ and NAOI (Fig. 6II), but the positive relationship is insignificant during the

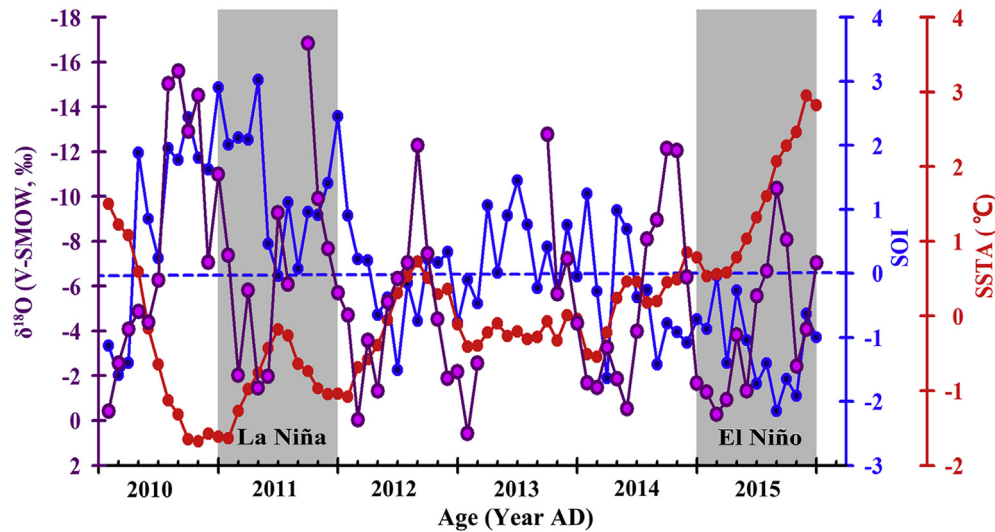


Fig. 5. The changes of the SSTA, SOI and precipitation $\delta^{18}\text{O}$ of Chongqing in 2010–2015. The gray bars denote the La Niña year (2011) and El Niño year (2015), respectively.

negative phase of NAOI. This positive relation is further confirmed by the precipitation $\delta^{18}\text{O}$ of Dhaka and Sylhet, Bangladesh (Fig. 6).

The correlation coefficient between the $\delta^{18}\text{O}$ of precipitation in Chongqing and NAOI in phase I, II, III and IV are 0.633, 0.773, 0.695 and 0.785, respectively, with the expectation in phase I, where there is a lag of 1–2 months between the precipitation $\delta^{18}\text{O}$ and the NAOI (Fig. 6). In the NAO strong years, over the North Atlantic, the pressure difference of sea surface between the mid-latitude subtropical High and the high-latitude subpolar Low increases, strengthening the westerlies and pushing it move northward (the gray zone in Fig. 7A) (Barnston and Livezey, 1987; Hurrell, 1995; Liu et al., 2015). The modeled result using the NCEP/NCAR (National Centers for Environmental Prediction/National Center for Atmospheric Research) reanalysis data, reported by the NOAA-ESRL (National Oceanic and Atmospheric Administration-Environment Systems Research Institute) Physical Sciences Division, Boulder Colorado on their Web site at <http://www.esrl.noaa.gov/psd/>, confirmed this conclusion (Fig. 8B, D, F, and H). In this situation,

Siberia is closer to the moisture source with heavier stable isotopic composition. On the other hand, the vapor for the winter precipitation in southwest China is dominated by the winter monsoon originated from the Siberia-Mongolia High (SMH). So, the $\delta^{18}\text{O}$ of precipitation in southwest China have the similar trend as the change of NAOI, with a phase lag of 1–2 months. When the NAOI decreases, the westerlies can be weakened and move southward (the gray zone in Figs. 7B and 8A, C, E, and G). Moisture from the Atlantic is converged nearby the Tianshan Mountains and leads to precipitation, so that there is no obvious correlation between the NAOI and the precipitation $\delta^{18}\text{O}$ of southwest, China.

4. Conclusions

In this study, based on a 6-year monitoring on the precipitation in Chongqing, southwest China, we analyzed the change of δD and $\delta^{18}\text{O}$ and assessed the relationships between the variation of $\delta^{18}\text{O}$ / δD , ENSO, and NAO. The main points were presented as below.

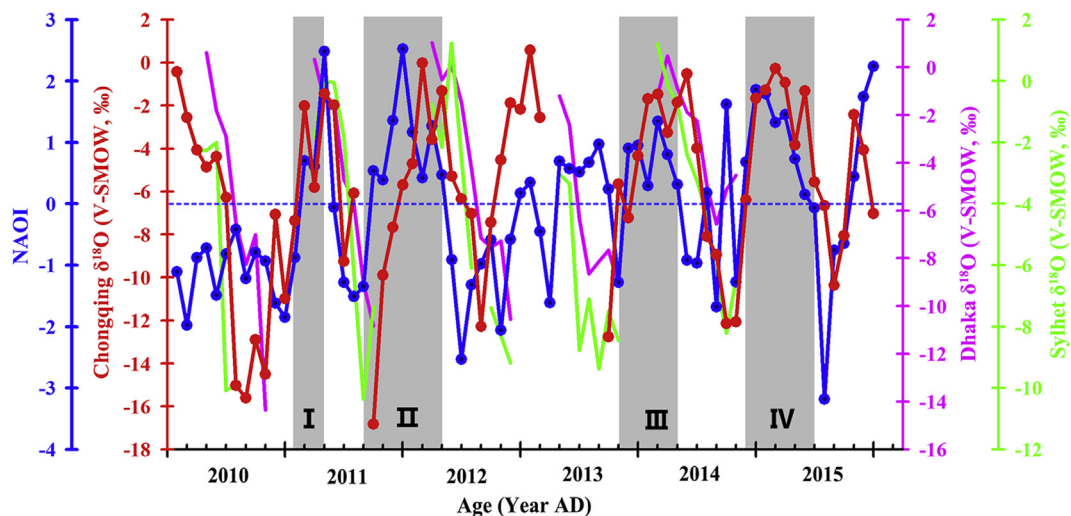


Fig. 6. Relationship between the NAOI and the precipitation $\delta^{18}\text{O}$ in Chongqing. The positive phase periods of NAOI (gray bars) are Feb. to Apr. 2011 (I), Sept. 2011 to Apr. 2012 (II), Nov. 2013 to Apr. 2014 (III) and Nov. 2014 to May 2015 (IV). The pink and the green lines present the $\delta^{18}\text{O}$ of precipitation in Dhaka and Sylhet, Bangladesh (Fig. 1), respectively (with some data lack). (For interpretation of the references to colour in this figure legend, the reader is referred to the web version of this article.)

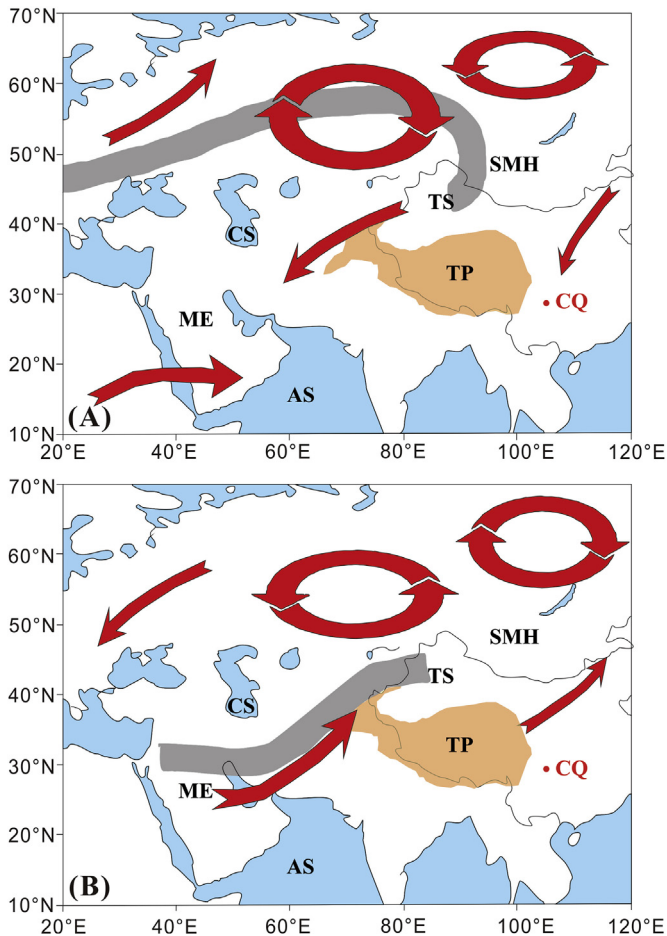


Fig. 7. Differences of the water vapor source for the Tianshan Mountains region in the westerlies moves northward and southward year (Simplified from Fig. 5 in Liu et al., 2015). (A) The westerlies move northward; B. The westerlies move southward. Gray band indicates the main pathway of water vapor source. CS: Caspian Sea; ME: Middle East; AS: Arabian Sea; TP: Tibetan Plateau; SMH: Siberia-Mongolia High; CQ: Chongqing City; TS: Tianshan Mts.) The red arrows indicate the flow of water vapor. (For interpretation of the references to colour in this figure legend, the reader is referred to the web version of this article.)

- (1) The LMWL and the LPWMWL equations of Chongqing are $\delta D = 8.33\delta^{18}O + 19.42$ and $\delta D = 8.30\delta^{18}O + 16.60$, respectively. Both the negative correlations between the $\delta D/\delta^{18}O$ values, temperature and rainfall, and the seasonal change of *d-excess* (decrease in summer and increase in winter), are mainly dominated by the seasonal change of moisture sources.
- (2) There is an obvious connection between the $\delta D/\delta^{18}O$ of precipitation in southwest China and ENSO. During the El Niño years, more vapor from the closer moisture source contributes to local precipitation, leading to a heavier stable isotopic composition of rainwater, but the situation in La Niña years is completely different, e.g. in 2011.
- (3) The northward/southward migration of the westerlies and the change of moisture pathways may connect the NAO and the change of precipitation isotopic composition in southwest China. When the NAOI is in the positive phase (always in boreal winter), there is a positive relationship between the $\delta^{18}O$ of precipitation in southwest China and the NAOI.
- (4) The conclusion about atmospheric circulations above is a tentative summary because the $\delta^{18}O$ data of Chongqing is just for 6 years, which is a relative short time for large-scale ocean-atmosphere general circulation model. More data for extensive region and longer time is essential to test the preliminary conclusion of this study.

Acknowledgement

Two anonymous reviewers and editor Hema Achyuthan are greatly appreciated for their constructive comments to improve the quality of this article. This work was supported by the National Science Foundation of China grants (Nos. 41172165 and 41440020), the Fundamental Research Funds for the Central Universities, Southwest University, China (XDJK2017A010, XDJK2013A012), to Li T.-Y. Dr. Xiang Xin-Yi, School of Geographical Sciences, Southwest University, China, is greatly appreciated for helping to polish the original English manuscript of this paper.

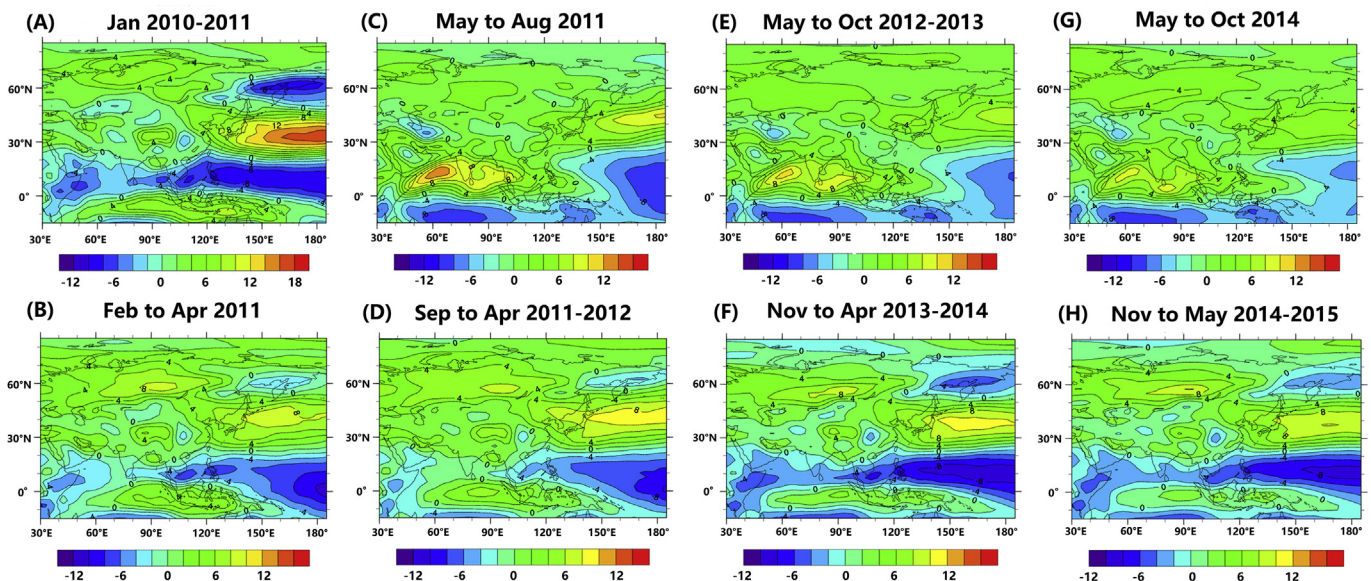
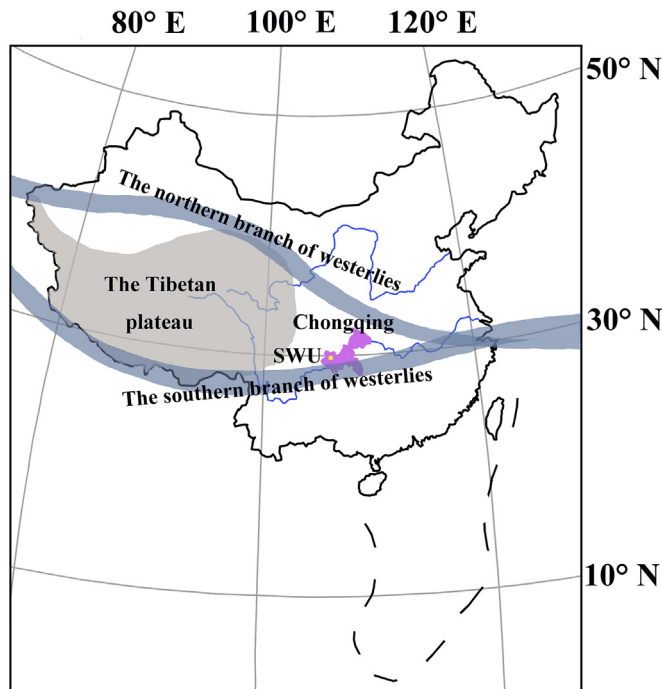


Fig. 8. The distribution of 850 mb zonal wind speed (m/s) in Asia during the negative/positive phase of NAOI (from Jan. 2010 to May 2015). The positive (negative) value of wind speed means the west (east) wind. In the negative phase of NAOI, westerlies moves southward and the speed increases in south area (A, C, E, G). While in the positive phase of NAOI, westerlies moves northward and the speed increases in north area (B, D, F, H).

Appendix



Appendix Fig. 1. The yellow dot indicates the location of the Southwest University (SWU) in Chongqing city (purple area), Southwest China. The gray area denotes the region of the Tibetan Plateau (TP) and the light blue bands present the northern and southern branch of the westerlies around the Tibetan Plateau.

Year/month	δD (V-SMOW, ‰)	Year/ month	δD (V-SMOW, ‰)	Year/ month	δD (V-SMOW, ‰)
201001	16.9	201201	-14.2	201401	10.7
201002	0.1	201202	18.9	201402	5.7
201003	-1.5	201203	-13.2	201403	-8.6
201004	-8.8	201204	1.2	201404	-1.7
201005	-9.1	201205	-24.7	201405	13.4
201006	-25.1	201206	-41.2	201406	-17.5
201007	-102.1	201207	-54.0	201407	-57.1
201008	-105.2	201208	-91.4	201408	-63.6
201009	-81.7	201209	-45.9	201409	-86.6
201010	-90.6	201210	-19.4	201410	-87.0
201011	-29.9	201211	2.9	201411	-33.5
201012	-53.8	201212	2.0	201412	14.0
201101	-17.7	201301	35.5	201501	11.3
201102	12.3	201302	3.1	201502	14.1
201103	-29.0	201303	-	201503	4.9
201104	-3.9	201304	-	201504	-16.6
201105	-0.1	201305	-	201505	4.0
201106	-64.5	201306	-	201506	-31.7
201107	-43.6	201307	-	201507	-42.4
201108	-	201308	-	201508	-74.0
201109	-122.3	201309	-91.1	201509	-51.1
201110	-71.2	201310	-28.1	201510	-6.9
201111	-45.1	201311	-41.4	201511	-14.8
201112	-21.8	201312	-11.4	201512	-37.5

Year/ month	$\delta^{18}O$ (V-SMOW, ‰)	Year/ month	$\delta^{18}O$ (V-SMOW, ‰)	Year/ month	$\delta^{18}O$ (V-SMOW, ‰)
201001	-0.43	201201	-4.71	201401	-1.69
201002	-2.57	201202	-0.03	201402	-1.48
201003	-4.08	201203	-3.59	201403	-3.25
201004	-4.86	201204	-1.32	201404	-1.85

(continued)

Year/ month	$\delta^{18}O$ (V-SMOW, ‰)	Year/ month	$\delta^{18}O$ (V-SMOW, ‰)	Year/ month	$\delta^{18}O$ (V-SMOW, ‰)
201005	-4.39	201205	-5.29	201405	-0.52
201006	-6.27	201206	-6.34	201406	-3.98
201007	-15.03	201207	-7.04	201407	-8.09
201008	-15.6	201208	-12.28	201408	-8.95
201009	-12.9	201209	-7.43	201409	-12.14
201010	-14.51	201210	-4.54	201410	-12.06
201011	-7.06	201211	-1.88	201411	-6.4
201012	-10.98	201212	-2.18	201412	-1.67
201101	-7.37	201301	0.58	201501	-1.27
201102	-2.01	201302	-2.56	201502	-0.28
201103	-5.82	201303	-	201503	-0.94
201104	-1.45	201304	-	201504	-3.83
201105	-1.98	201305	-	201505	-1.33
201106	-9.26	201306	-	201506	-5.56
201107	-6.09	201307	-	201507	-6.67
201108	-	201308	-	201508	-10.36
201109	-16.83	201309	-12.77	201509	-8.07
201110	-9.9	201310	-5.66	201510	-2.43
201111	-7.67	201311	-7.22	201511	-4.08
201112	-5.69	201312	-4.34	201512	-7.03

Year/ month	d-excess (‰)	Year/ month	d-excess (‰)	Year/ month	d-excess (‰)
201001	20.31	201201	23.47	201401	24.23
201002	20.65	201202	19.18	201402	17.54
201003	31.15	201203	15.49	201403	17.41
201004	30.05	201204	11.81	201404	13.14
201005	26.03	201205	17.61	201405	17.61
201006	25.08	201206	9.58	201406	14.35
201007	18.1	201207	2.25	201407	7.62
201008	19.58	201208	6.88	201408	8.02
201009	21.5	201209	13.61	201409	10.53
201010	25.51	201210	16.93	201410	9.48
201011	26.58	201211	17.95	201411	17.68
201012	34.08	201212	19.41	201412	27.32
201101	41.24	201301	30.89	201501	21.47
201102	28.37	201302	23.53	201502	16.35
201103	17.54	201303	-	201503	12.46
201104	7.71	201304	-	201504	14.04
201105	15.79	201305	-	201505	14.65
201106	9.67	201306	-	201506	12.82
201107	5.09	201307	-	201507	10.96
201108	-	201308	-	201508	8.81
201109	12.39	201309	11.05	201509	13.48
201110	8.01	201310	17.2	201510	12.58
201111	16.3	201311	16.36	201511	17.77
201112	23.77	201312	23.35	201512	18.74

Year/ month	T (°C)	P (mm)	Year/ month	T (°C)	P (mm)	Year/ month	T (°C)	P (mm)
201001	8.8	12.6	201201	7.2	26.5	201401	7.8	8.4
201002	10.3	10	201202	8.6	12.9	201402	8.7	11.7
201003	14.1	44.2	201203	13.7	25.4	201403	14.1	121.8
201004	16.6	129.7	201204	19.7	56.2	201404	19.3	95.8
201005	21.8	117	201205	22.5	230.3	201405	20.6	114.2
201006	23.9	100.4	201206	24.3	164.6	201406	23.7	223.4
201007	28.9	209.6	201207	28	113.1	201407	28.7	132.3
201008	28.7	55.9	201208	29	97.1	201408	26.9	203.8
201009	25.1	90	201209	22.8	145.9	201409	23.9	303.8
201010	18.1	48.8	201210	17.9	70.5	201410	19.9	100.6
201011	14.2	53.1	201211	13.1	25.7	201411	13.7	64.6
201012	8.1	28.6	201212	9.1	8.1	201412	8.6	12.9
201101	4.7	18.1	201301	7.8	6	201501	9.2	14.5
201102	9.8	9.8	201302	11.6	17.5	201502	11.1	6
201103	11.5	46.3	201303	17.7	4.9	201503	15.8	25.4
201104	19.2	122.2	201304	20.1	91.7	201504	20.1	80.1
201105	23.3	114.5	201305	22.3	306.2	201505	22.5	120.9

(continued on next page)

(continued)

Year/ month	T (°C)	P (mm)	Year/ month	T (°C)	P (mm)	Year/ month	T (°C)	P (mm)
201106	26.2	156.9	201306	27.5	278.7	201506	25.4	301.4
201107	28.7	70.6	201307	30.6	88.9	201507	27.5	149.3
201108	30.5	31.2	201308	29.5	103	201508	26.9	260.2
201109	24.1	55.6	201309	23	170.7	201509	23.6	222.5
201110	18.9	147.9	201310	19.1	84.1	201510	19.9	81
201111	16.1	94.9	201311	14.1	53	201511	15.8	19
201112	8.7	42.1	201312	8.5	17.6	201512	9.7	31.2

References

- Allan, R.J., Nicholls, N., Jones, P.D., Butterworth, I.J., 1991. A further extension of the Tahiti-Darwin SOI, early ENSO events and Darwin pressure. *J. Clim.* 4 (7), 743–749.
- Barnston, A.G., Livezey, R.E., 1987. Classification, seasonality and persistence of low-frequency atmospheric circulation patterns. *Mon. Weather Rev.* 115 (6), 1083–1126.
- Bjerknes, J., 1969. Atmospheric teleconnections from the equatorial Pacific. *Mon. Weather Rev.* 97 (3), 163–172.
- Brandimarte, L., Baldassarre, G.D., Bruni, G., D'Odorico, P., Montanari, A., 2011. Relation between the North-Atlantic oscillation and hydroclimatic conditions in Mediterranean areas. *Water Resour. Manag.* 25 (5), 1269–1279.
- Cai, Y.J., Fung, I.Y., Edwards, R.L., An, Z.S., Cheng, H., Lee, J.E., Tan, L.C., Shen, C.C., Wang, X.F., Day, J.A., Zhou, W.J., Kelly, M.J., Chiang, J.C.H., 2015. Variability of stalagmite-inferred Indian monsoon precipitation over the past 252,000y. *Proc. Natl. Acad. Sci.* 112 (10), 2954–2959.
- Cane, M.A., 2005. The evolution of El Niño, past and future. *Earth Planet. Sci. Lett.* 230 (3), 227–240.
- Chen, F.L., Zhang, M.J., Wang, S.J., Ma, Q., Zhu, X.F., Dong, L., 2015. Relationship between sub-cloud secondary evaporation and stable isotopes in precipitation of Lanzhou and surrounding area. *Quat. Int.* 380–381, 68–74.
- Cheng, H., Sinha, A., Wang, X.F., Cruz, F.W., Edwards, R.L., 2012. The global paleomonsoon as seen through speleothem records from Asia and the Americas. *Clim. Dyn.* 39 (5), 1045–1062.
- Coplen, T.B., Neiman, P.J., White, A.B., Landwehr, J.M., Ralph, F.M., Dettlinger, M.D., 2008. Extreme changes in stable hydrogen isotopes and precipitation characteristics in a landfalling Pacific storm. *Geophys. Res. Lett.* 35 (21), 154–171.
- Craig, H., 1961. Isotopic variations in meteoric waters. *Science* 133 (3465), 1702–1703.
- Cui, Y.F., Duan, A.M., Liu, Y.M., Wu, G.X., 2015. Inter-annual variability of the spring atmospheric heat source over the Tibetan Plateau forced by the North Atlantic SSTA. *Clim. Dyn.* 45 (5–6), 1617–1634.
- Dansgaard, W., 1964. Stable isotopes in precipitation. *Tellus* 16 (4), 436–468.
- Deshpande, R.D., Maurya, A.S., Kumar, B., Sarkar, A., Gupta, S.K., 2013. Kinetic fractionation of water isotopes during liquid condensation under super-saturated condition. *Geochim. Cosmochim. Acta* 100 (1), 60–72.
- Ding, Y.H., Liu, Y.Y., 2008. A study of the teleconnections in the Asian-Pacific monsoon region. *Acta Meteorol. Sin.* 22 (4), 404–418.
- Duan, W.H., Ruan, J.Y., Luo, W.J., Li, T.Y., Tian, L.J., Zeng, G.N., Zhang, D.Z., Bai, Y.J., Li, J.L., Tao, T., Zhang, P.Z., Baker, A., Tan, M., 2016. The transfer of seasonal isotopic variability between precipitation and drip water at eight caves in the monsoon regions of China. *Geochim. Cosmochim. Acta* 183, 250–266.
- Dvoryaninov, G.S., Kubryakov, A.A., Sizov, A.A., Stanichny, S.V., Shapiro, N.B., 2016. The North Atlantic Oscillation: a dominant factor in variations of oceanic circulation systems of the Atlantic Ocean. *Dokl. Earth Sci.* 466 (1), 100–104.
- Eastoe, C.J., Dettman, D.L., 2016. Isotope amount effects in hydrologic and climate reconstructions of monsoon climates: implications of some long-term data sets for precipitation. *Chem. Geol.* 430, 78–89.
- Fritz, P., Drimmie, R.J., Frapce, S.K., O'Shea, K., 1987. The isotopic composition of precipitation and groundwater in Canada. *Atmos. Precip.* 539–550.
- Ham, Y.G., Kug, J.S., 2014. Effects of Pacific Intertropical Convergence Zone precipitation bias on ENSO phase transition. *Environ. Res. Lett.* 9 (6), 64008–64015.
- Han, L.-Y., Li, T.-Y., Cheng, H., Edwards, R.L., Shen, C.-C., Li, H.-C., Huang, C.-X., Li, J.-Y., Yuan, N., Wang, H.-B., Zhang, T.-T., Zhao, X., 2016. Potential influence of temperature changes in the southern hemisphere on the evolution of the Asian summer monsoon during the last glacial period. *Quat. Int.* 392, 239–250.
- Hoffmann, G., Jouzel, J., Masson, V., 2000. Stable water isotopes in atmospheric general circulation models. *Hydrol. Process.* 14 (8), 1385–1406.
- Hughes, C.E., Crawford, J., 2012. A new precipitation weighted method for determining the meteoric water line for hydrological applications demonstrated using Australian and global GNIP data. *J. Hydrol.* 464–465 (13), 344–351.
- Hurrell, J.W., 1995. Decadal trends in the North Atlantic Oscillation: regional temperatures and precipitation. *Science* 269, 676–679.
- Kebede, S., Travi, Y., 2012. Origin of the $\delta^{18}\text{O}$ and δD composition of meteoric waters in Ethiopia. *Quat. Int.* 257, 4–12.
- Lechler, A.R., Niemi, N.A., 2011. Controls on the spatial variability of modern meteoric $\delta^{18}\text{O}$: empirical constraints from the Western US and East Asia and implications for stable isotope studies. *Mod. Asian Stud.* 10 (1), 41–64.
- Li, T.-Y., Li, H.-C., Shen, C.-C., Yang, C.-X., Li, J.-Y., Yi, C.-C., Yuan, D.-X., Wang, J.-L., Xie, S.-Y., 2010. Study on the δD and $\delta^{18}\text{O}$ characteristics of meteoric precipitation during 2006–2008 in Chongqing China. *Adv. Water Sci.* 21 (6), 757–764 (in Chinese).
- Li, T.-Y., Shen, C.-C., Huang, L.-J., Jiang, X.-Y., Yang, X.-L., Mii, H.-S., Li, L., 2014. Stalagmite-inferred variability of the Asian Summer monsoon during the penultimate glacial-interglacial period. *Clim. Past* 10 (3), 1211–1219.
- Liu, H.C., Duan, K.Q., 2012. Effects of North Atlantic oscillation on summer precipitation over the Tibetan plateau. *J. Glaciol. Geocryol.* 34 (2), 311–318 (in Chinese).
- Liu, X., Yin, Z.Y., 2001. Spatial and temporal variation of summer precipitation over the eastern Tibetan plateau and the North Atlantic oscillation. *J. Clim.* 14 (13), 2896–2909.
- Liu, J.R., Song, X.F., Yuan, G.F., Sun, X.M., Liu, X., Chen, F., Wang, Z.M., Wang, S.Q., 2008. Characteristics of $\delta^{18}\text{O}$ in precipitation over northwest China and its water vapor sources. *Acta Geogr. Sin.* 63 (1), 12–22.
- Liu, J.R., Song, X.F., Yuan, G.F., Sun, X.M., Wang, S.Q., 2010. Characteristics of $\delta^{18}\text{O}$ in precipitation over Eastern Monsoon China and the water vapor sources. *Chin. Sci. Bull.* 55 (2), 200–211.
- Liu, X.K., Rao, Z.G., Zhang, X.J., Wei, H., Chen, J.H., Chen, F.H., 2015. Variations in the oxygen isotopic composition of precipitation in the Tianshan mountains region and their significance for the westerly circulation. *J. Geogr. Sci.* 25 (7), 801–816.
- Marshall, J., Kushnir, Y., Battisti, D., Chang, P., Czaja, A., Dickson, R., Hurrell, J.W., McCartney, M., Saravanan, R., Visbeck, M., 2001. North Atlantic climate variability: phenomena, impacts and mechanisms. *Int. J. Climatol.* 21 (15), 1863–1898.
- Merlivat, L., Jouzel, J., 1979. Global climatic interpretation of the deuterium-oxygen 18 relationship for precipitation. *J. Geophys. Res. Oceans* 84 (C8), 5029–5033.
- Neelin, J.D., Battisti, D.S., Hirst, A.C., Jin, F.F., Wakata, Y., Yamagata, T., Zebiak, S.E., 1998. ENSO theory. *J. Geophys. Res. Oceans* 1031 (C7), 14261–14290.
- Pang, H.X., He, Y.Q., Zhang, Z.L., 2005. Correlation between deuterium excess in monsoon precipitation of New Delhi and the origin of precipitation. *J. Glaciol. Geocryol.* 27 (6), 876–880.
- Peng, S., Robinson, W.A., Li, S., 2002. North Atlantic SST forcing of the NAO and relationships with intrinsic hemispheric variability. *Geophys. Res. Lett.* 29 (8), 117–111.
- Railsback, L.B., Xiao, H.L., Liang, F.Y., Akers, P.D., Brook, G.A., Dennis, W.M., Lanier, T.E., Tan, M., Cheng, H., Edwards, R.L., 2014. A stalagmite record of abrupt climate change and possible Westerlies-derived atmospheric precipitation during the Penultimate Glacial Maximum in northern China. *Palaeogeogr. Palaeoclimatol. Palaeoecol.* 393 (2), 30–44.
- Rogers, J.C., 1984. The association between the North Atlantic oscillation and the southern oscillation in the Northern hemisphere. *Mon. Weather Rev.* 112, 1999–2015.
- Ropelewski, C.F., Jones, P.D., 1987. An extension of the Tahiti-Darwin southern oscillation index. *Mon. Weather Rev.* 115 (9), 2161–2165.
- Rozanski, K., Araguás-Araguás, L., Gonfiantini, R., 1993. Isotopic patterns in modern global precipitation. *Wash. D.C. Am. Geophys. Union Geophys. Monogr.* 78, 1–36.
- Serreze, M.C., Carse, F., Barry, R.G., Rogers, J.C., 1995. Icelandic low cyclone activity: climatological features, linkages with the NAO, and relationships with recent changes in the northern hemisphere circulation. *J. Clim.* 10 (3), 453–464.
- Song, X.F., Liu, J.R., Sun, X.M., Yuan, G.F., Liu, X., Wang, S.Q., Hou, S.B., 2007. Establishment of Chinese Network of isotopes in precipitation (CHNIP) based on CERN. *Adv. Earth Sci.* 22 (7), 738–747 (in Chinese).
- Strong, M., Sharp, Z.D., Gutzler, D.S., 2007. Diagnosing moisture transport using D/H ratios of water vapor. *Geophys. Res. Lett.* 34 (3), 340–354.
- Stumpp, C., Klaus, J., Stiehler, W., 2014. Analysis of long-term stable isotopic composition in German precipitation. *Br. J. Addict. Alcohol & Other Drugs* 517 (4), 351–361.
- Takahashi, K., Onodera, J., Katsurada, Y., 2009. Relationship between time-series diatom fluxes in the central and western equatorial Pacific and ENSO-associated migrations of the Western Pacific Warm Pool. *Deep Sea Res. Part I Oceanogr. Res. Pap.* 56 (8), 1298–1318.
- Tan, M., 2009. Circulation effect: climatic significance of the short term variability of the oxygen isotopes in stalagmites from monsoonal China – dialogue between paleoclimate records and modern climate research. *Quat. Sci.* 29 (5), 851–862 (in Chinese).
- Tan, M., 2014. Circulation effect: response of precipitation $\delta^{18}\text{O}$ to the ENSO cycle in monsoon regions of China. *Clim. Dyn.* 42 (3–4), 1067–1077.
- Tan, M., 2016. Circulation background of climate patterns in the past millennium: uncertainty analysis and re-reconstruction of ENSO-like state. *Sci. China Earth Sci.* (6), 1–17.
- Tian, L.D., Yao, T.D., Sun, W.Z., Stievenard, M., Jouzel, J., 2001. Relationship between δD and $\delta^{18}\text{O}$ in precipitation on north and south of the Tibetan Plateau and moisture recycling. *Sci. China Earth Sci.* 44 (9), 789–796.
- Tian, L.D., Yao, T.D., White, J.W.C., Yu, W.S., Wang, N.L., 2005. Westerly moisture transport to the middle of Himalayas revealed from the high deuterium excess. *Chin. Sci. Bull.* 50 (10), 1026–1030.
- Tian, L.D., Yao, T.D., MacLune, K., White, J.W.C., Schilla, A., Vaughn, B., Vachon, R., Ichiyonagi, K., 2007. Stable isotopic variations in west China: a consideration of moisture sources. *J. Geophys. Res. Atmos.* 112, D10112.

- Trenberth, K.E., 1997. The definition of El Niño. *Bull. Am. Meteorol. Soc.* 78 (12), 2771–2777.
- Walker, G.T., 1925. Correlation in seasonal variations of weather—a further study of world weather. *Q. J. R. Meteorol. Soc.* 20 (571), 1–24.
- Wang, B., Wu, R., Fu, X., 2000. Pacific-East Asian teleconnection: how does ENSO affect East Asian climate? *J. Clim.* 13 (9), 1517–1536.
- Wang, Y.J., Cheng, H., Edwards, R.L., An, Z.S., Wu, J.Y., Shen, C.C., Dorale, J.A., 2001. A high-resolution absolute-dated late Pleistocene monsoon record from Hulu cave, China. *Science* 294 (5550), 2345–2348.
- Wang, X.Y., Li, Z.Q., Tayler, R., Wang, S.J., 2015. Characteristics of atmospheric precipitation isotopes and isotopic evidence for the moisture origin in Yushugou river basin, Eastern Tianshan Mountains, China. *Quat. Int.* 380–381, 106–115.
- Watanabe, M., 2004. Asian jet waveguide and a downstream extension of the North Atlantic Oscillation. *J. Clim.* 17 (24), 4674–4691.
- Xu, H.L., Li, J.P., Feng, J., Mao, J.Y., 2012. The asymmetric relationship between the winter NAO and the precipitation in Southwest China. *Acta Meteorol. Sin.* 70 (6), 1276–1291 (in Chinese).
- Yang, H., Johnson, K.R., Griffiths, M.L., Yoshimura, K., 2016. Interannual controls on oxygen isotope variability in Asian monsoon precipitation and implications for paleoclimate reconstructions. *J. Geophys. Res. Atmos.* 121 (14), 8410–8428.
- Zhang, X.P., Liu, J.M., Tian, L.D., He, Y.Q., Yao, T.D., 2004. Variations of $\delta^{18}\text{O}$ in precipitation along vapor transport paths. *Adv. Atmos. Sci.* 21 (4), 562–572.
- Zhang, L., Chen, L., Liu, J., Liu, F.L., Chen, Z.Y., 2009a. D and ^{18}O isotopes in atmospheric precipitation in Hongkong area. *Ecol. Environ. Sci.* 18 (2), 572–577 (in Chinese).
- Zhang, X.P., Liu, J.M., Masayishi, N., Xie, Z.C., 2009b. Vapor origins revealed by deuterium excess in precipitation in southwest China. *J. Glaciol. Geocryol.* 31 (4), 613–619 (in Chinese).
- Zheng, S.H., Hou, F.G., Ni, B.L., 1983. Study on the hydrogen and oxygen stable isotopes in meteoric precipitation of China. *Chin. Sci. Bull.* 13, 801–806 (in Chinese).
- Zhang, T.-T., Li, T.-Y., Cheng, H., Edwards, R.L., Shen, C.-C., Spötl, C., Li, H.-C., Han, L.-Y., Li, J.-Y., Huang, C.-X., Zhao, X., 2017. Stalagmite-inferred centennial variability of the Asian summer monsoon in southwest china between 58 and 79 ka BP. *Quat. Sci. Rev.* 160, 1–12.
- Zhou, T.J., Yu, R.C., 2005. Atmospheric water vapor transport associated with typical anomalous summer rainfall patterns in China. *J. Geophys. Res. Atmos.* 110 (D8), D08104.
- Zhou, S.Q., Nakawo, M., Sakai, A., Matsuda, Y., Duan, K.Q., Pu, J.C., 2007. Water isotope variations in the snow pack and summer precipitation at July 1 Glacier, Qilian Mountains in Northwest China. *Chin. Sci. Bull.* 52 (21), 2963–2972.